CALIBRATION OF A POLARIZATION DIVERSE ARRAY

Hasan S. Mir

University of Washington, Seattle
hmir@mit.edu

John D. Sahr

University of Washington, Seattle
jdsahr@washington.edu

ABSTRACT

Direction finding (DF) performance is assessed for an array of airborne vector sensors whose manifold is perturbed. A calibration algorithm explicitly accounting for the polarization diverse nature of the vector sensor is developed. DF performance improvements are demonstrated with use of the proposed calibration algorithm.

1. INTRODUCTION

Conventional arrays consist of identical sensor elements, each of which samples a scalar projection of one of the electromagnetic fields. In contrast, a polarization diverse array includes sensors which sample different projections of the fields. Some of the sensors may have the same phase center, enabling estimation of the polarization state as well as the Poynting vector. A nominal vector sensor consists of two orthogonal triads of dipole and loop antennas, as shown in Figure 1.

A key application of sensor arrays is the passive localization of a radiating signal source. The sensor-to-sensor delays contain information about the source location in terms of the source azimuth angle θ and source elevation angle ϕ for two dimensional array configurations. This information is exploited in direction finding (DF) algorithms that estimate the source angle-of-arrival (AOA). DF algorithms utilize an underlying model which presumes a coherent phase relationship among the antenna array elements. Such a relationship almost never occurs in practice due to various anomalies such as sensor pattern variations and multipath propagation effects. Thus, array calibration, which attempts to fit the actual array response to the theoretical response, is essential for obtaining accurate DF estimates.

The angular resolution of an array is directly related to the size of its aperture. For airborne applications in which a sensor array is mounted on a small aircraft, the physical space available on the airframe is limited and as such, the array aperture is restricted.

Usage of a vector sensor for source localization was first proposed in [1]. The rationale is that because a vector sensor uses multiple components of electromagnetic information, it can offer accurate source location estimates with a smaller aperture. Indeed, if a full vector sensor (which measures the complete electric and magnetic fields) with an arbitrarily small aperture provides sufficient sensitivity, the source location can be estimated by simply calculating the Poynting vector. Thus, vector sensors are useful in situations wherein the available physical space is constrained.

In the following sections, a novel calibration algorithm designed specifically for a polarization diverse array is developed. This calibration algorithm is motivated by the observation that the polarization state is parameterized by a linear two-dimensional subspace [2]. The remainder of this paper is organized as follows- Section 2 develops the signal model for a polarization diverse array. Section 3 formulates the proposed polarization diverse calibration algorithm. Section 4 presents the simulation results and discussion.

2. SIGNAL MODEL FORMULATION

Initial studies with a vector sensor mounted on an aircraft indicated that some elements of the vector sensor act as "feeds" and are strongly coupled to the airframe, reducing their usefulness for DF purposes. The proposed solution to the problem is to use a "trimmed" vector sensor employing only the elements with insignificant airframe interaction. Multiple trimmed vector sensors are sited at strategic locations on the airframe, providing increased aperture for accurate AOA estimates.

A particular trimmed 8-channel vector sensor configuration studied in this paper is shown in Figure 1. The two loop antennas measure the x and y components of the magnetic field, while the vertical dipole measures the z component of the electric field. In view of aerodynamic issues and the varying sensor interaction at different locations on the airframe, the trimmed vector sensors on the aircraft are not all

This work was sponsored by the Department of Defense under Air Force Contract F19628-00-C-0002. Opinions, interpretations, conclusions, and recommendations are those of the authors and are not necessarily endorsed by the United States Government.

The authors acknowledge the work of Dan Bliss, Amanda Chan, and Alex Eapen for their modeling work to establish an appropriate vector sensor array for a small aircraft.

identical; the one mounted on the tip of the airframe lacks the vertical dipole.

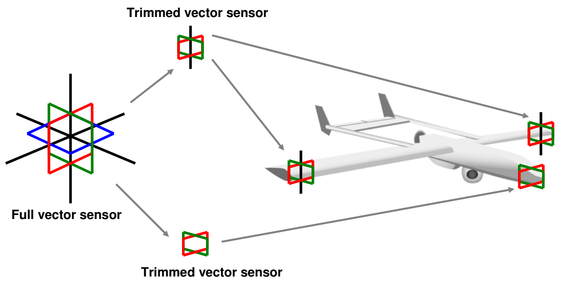

Fig. 1. A full vector sensor and its decompostion into trimmed vector sensors. The 8-channel aircraft configuration consists of identical 3-channel sensors mounted on the wings, and a 2-channel sensor mounted on the tip.

2.1. Signal Model

It is assumed in this paper that the vector sensor array is in the far-field of a narrowband signal.

Following [3], define the components of the electric and magnetic field received on the array as

$$\begin{bmatrix} E_x \\ E_y \\ E_z \\ H_x \\ H_y \\ H_z \end{bmatrix} = \begin{bmatrix} \cos(\theta)\cos(\phi) & -\sin(\theta) \\ \sin(\theta)\cos(\phi) & \cos(\theta) \\ -\sin(\phi) & 0 \\ -\sin(\theta) & -\cos(\theta)\cos(\phi) \\ \cos(\theta) & -\sin(\theta)\cos(\phi) \\ 0 & \sin(\phi) \end{bmatrix} \begin{bmatrix} \sin(\gamma) e^{+j\eta} \\ \cos(\gamma) \end{bmatrix}$$

$$= \boldsymbol{\Theta}(\theta,\phi)\,\mathbf{p}(\gamma,\eta) \tag{1}$$

where $\boldsymbol{\Theta}(\theta,\phi)$ and $\mathbf{p}(\gamma,\eta)$ are defined appropriately, and $0^\circ \le \gamma \le 180^\circ$ and $-180^\circ \le \eta \le 180^\circ$ are the ranges of the polarization angle and phase difference, respectively. It should be pointed out that the additional polarization state parameters γ and η are now required to index the array manifold, along with the previously defined conventional AOA parameters θ and ϕ. However, knowledge of γ and η is generally not of interest, and they are thus considered to be nuisance parameters.

Let $\mathbf{r}_m$ be a location matrix for sensors of a particular type, and let $\boldsymbol{\Theta}_m(\theta,\phi)$ be the appropriate row of $\boldsymbol{\Theta}(\theta,\phi)$ corresponding to the particular field component that the sensors measure. Define a unit vector in the source direction

$$\mathbf{u}(\theta,\phi) = \begin{bmatrix} \cos(\theta)\sin(\phi) & \sin(\theta)\sin(\phi) & \cos(\phi) \end{bmatrix}^T \tag{2}$$

The plane wave (far-field) response is defined as

$$\mathbf{v}_m(\theta,\phi) = e^{+j\frac{2\pi}{\lambda}\mathbf{r}_m^T\mathbf{u}(\theta,\phi)} \tag{3}$$

where λ is the signal wavelength.

The response/steering vector of the vector sensor array is generated by concatenating the response of identical sensor types

$$\mathbf{v}_{\mathrm{vs}}(\theta,\phi,\gamma,\eta) = \begin{bmatrix} \mathbf{v}_{\mathrm{vs},1}(\theta,\phi,\gamma,\eta) \\ \vdots \\ \mathbf{v}_{\mathrm{vs},M}(\theta,\phi,\gamma,\eta) \end{bmatrix} \tag{4}$$

where

$$\mathbf{v}_{\mathrm{vs},m}(\theta,\phi,\gamma,\eta) = \mathbf{v}_m(\theta,\phi)\left[\boldsymbol{\Theta}_m(\theta,\phi)\,\mathbf{p}(\gamma,\eta)\right] \tag{5}$$

and M is the number of distinct field components being measured, or equivalently, the number of different sensor types.

For the trimmed vector sensor configuration shown in Figure 1 measuring the three components H_x, H_y, and E_z, the value of M equals 3. Letting v_{lw}, v_{rw}, and v_{t} represent the plane wave response for the sensors on the left wing, right wing, and tip of the aircraft, respectively, the trimmed vector sensor response becomes

$$\mathbf{v}_{\mathrm{vs}}(\theta,\phi,\gamma,\eta) = \begin{bmatrix} \begin{pmatrix} v_{\mathrm{lw}} \\ v_{\mathrm{rw}} \end{pmatrix} E_z \\ \begin{pmatrix} v_{\mathrm{lw}} \\ v_{\mathrm{rw}} \\ v_{\mathrm{t}} \end{pmatrix} H_x \\ \begin{pmatrix} v_{\mathrm{lw}} \\ v_{\mathrm{rw}} \\ v_{\mathrm{t}} \end{pmatrix} H_y \end{bmatrix}$$

which is indeed an 8×1 steering vector.

3. ARRAY CALIBRATION

Suppose an N element sensor array observes a stationary, far-field, narrowband source at K known and distinct look angles. Let $\mathbf{v}(\theta_k,\phi_k)$ and $\mathbf{z}(\theta_k,\phi_k)$ represent the $N \times 1$ modeled and measured array steering vector, respectively, for the source azimuth AOA θ_k and elevation AOA ϕ_k, where $k = 1 \ldots K$.

Define

$$\mathbf{V}(\boldsymbol{\theta},\boldsymbol{\phi}) \triangleq \begin{bmatrix} \mathbf{v}(\theta_1,\phi_1) & \ldots & \mathbf{v}(\theta_K,\phi_K) \end{bmatrix}$$

and

$$\mathbf{Z}(\boldsymbol{\theta},\boldsymbol{\phi}) \triangleq \begin{bmatrix} \mathbf{z}(\theta_1,\phi_1) & \ldots & \mathbf{z}(\theta_K,\phi_K) \end{bmatrix}$$

where $\boldsymbol{\theta}$ and $\boldsymbol{\phi}$ are vectors whose kth elements are θ_k and ϕ_k, respectively.

In the following development, conventional array calibration is introduced in order to augment its expansion into a calibration algorithm that explicitly accounts for the polarization diverse nature of the vector sensor.

3.1. Conventional Array Calibration Algorithm

Conventional array calibration seeks to compute a calibration matrix $\mathbf{A} \in \mathbb{C}^{N \times N}$ so that $\mathbf{z}(\theta_k, \phi_k) \approx \mathbf{A}\mathbf{v}(\theta_k, \phi_k)$.

One approach to compute the calibration matrix $\mathbf{A}$ is to use the least squares criterion [4]

$$\arg\min_{\mathbf{A}} J_{CA} \tag{6}$$

where

$$J_{CA} = \left\| \mathbf{Z}(\boldsymbol{\theta}, \boldsymbol{\phi}) - \mathbf{A}\mathbf{V}(\boldsymbol{\theta}, \boldsymbol{\phi}) \right\|_F^2 \tag{7}$$

and the subscript F denotes the Frobenius norm. The optimal solution for the calibration matrix is computed as

$$\mathbf{A} = \mathbf{Z}(\boldsymbol{\theta}, \boldsymbol{\phi}) \mathbf{V}^{\#}(\boldsymbol{\theta}, \boldsymbol{\phi}) \tag{8}$$

where $^{\#}$ denotes the Moore-Penrose pseudoinverse.

It is shown in [4] that this calibration algorithm (which does not assume polarization diversity of the array) yields noticeable performance gains when used with a conventional array. This calibration algorithm can also be applied to a polarization diverse array, with reasonable expectation for some performance gain. However, further performance improvement may be possible if a calibration algorithm explicitly accounting for the polarization diverse nature of the vector sensor is employed. This idea is now further explored.

3.2. Proposed Polarization Diverse Array Calibration Algorithm

Let $\mathbf{A}_1$ and $\mathbf{A}_2$ represent the calibration matrices for two distinct polarization states, and define

$$\mathbf{A}_D \triangleq \begin{bmatrix} \mathbf{A}_1 & \mathbf{A}_2 \end{bmatrix} \tag{9}$$

Furthermore, define a matrix of polarization state coefficients

$$\mathbf{P} = \begin{bmatrix} \vec{\mathbf{1}}_N \otimes \begin{bmatrix} c_{11} & \dots & c_{1K} \end{bmatrix} \\ \vec{\mathbf{1}}_N \otimes \begin{bmatrix} c_{21} & \dots & c_{2K} \end{bmatrix} \end{bmatrix} \tag{10}$$

The calibration may now be posed as the following optimization problem

$$\arg\min_{c_{1k}, c_{2k}, \mathbf{A}_1, \mathbf{A}_2} J_{PDA} \tag{11}$$

where

$$J_{PDA} \triangleq \left\| \mathbf{Z}(\boldsymbol{\theta}, \boldsymbol{\phi}) - \mathbf{A}_D \left[\mathbf{P} \odot \left(\vec{\mathbf{1}}_2 \otimes \mathbf{V}(\boldsymbol{\theta}, \boldsymbol{\phi}) \right) \right] \right\|_F^2 \tag{12}$$

The symbols $\odot$ and $\otimes$ denote the Hadamard and Kronecker product, respectively. The optimal solution for the calibration matrices (in the least squares sense) is

$$\mathbf{A}_D = \mathbf{Z}(\boldsymbol{\theta}, \boldsymbol{\phi}) \left[\mathbf{P} \odot \left(\vec{\mathbf{1}}_2 \otimes \mathbf{V}(\boldsymbol{\theta}, \boldsymbol{\phi}) \right) \right]^{\#} \tag{13}$$

$$\mathbf{c}_k \triangleq \begin{bmatrix} c_{1k} \\ c_{2k} \end{bmatrix} = \begin{bmatrix} \mathbf{A}_1 \mathbf{v}(\theta_k, \phi_k) & \mathbf{A}_2 \mathbf{v}(\theta_k, \phi_k) \end{bmatrix}^{\#} \mathbf{z}(\theta_k, \phi_k) \tag{14}$$

The optimal calibration parameters can now be computed by iterating between (13) and (14). For a selected tolerance ϵ, a criterion such as $\frac{1}{2N^2} \left\| \mathbf{A}_D^{(i)} - \mathbf{A}_D^{(i-1)} \right\|_F \leq \epsilon$, where $\mathbf{A}_D^{(i)}$ is the estimate of $\mathbf{A}_D$ at the ith iteration, can be used to terminate the iterations.

It should be noted that it is not necessary to search over $\mathbf{c}_k$ in a DF algorithm. Indeed, when the DF estimator (such as MuSIC) is cast as a Rayleigh quotient, $\mathbf{c}_k$ can be computed as simply an extremal eigenvector. The dimensionality of the search space as such remains unchanged.

4. SIMULATION RESULTS

The trimmed vector sensor configuration in Figure 1 is used for simulation studies. The aircraft geometry at 90 MHz is shown in Figure 2. Sensor manifold perturbations are

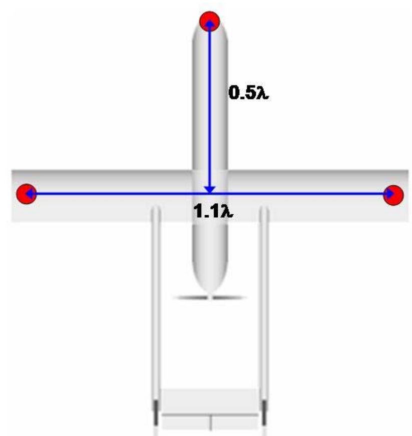

Fig. 2. Small aircraft geometry at 90 MHz with 3 trimmed vector sensor sites (c.f. Figure 1).

assumed to be caused by near-field scatterers local to the airframe. For every look angle k, the measured steering vector $\mathbf{z}(\theta_k, \phi_k)$ is modeled as follows:

$$\mathbf{z}(\theta_k, \phi_k) = \mathbf{v}_{\text{vs}}(\theta_k, \phi_k) + \varepsilon \sum_{s=1}^{N_{\text{scat}}} \mathbf{v}_{\text{mp},s} \tag{15}$$

where

$$\mathbf{v}_{\text{mp},s} = \begin{bmatrix} \mathbf{v}_1(\theta_s, \phi_s) \left[\boldsymbol{\Theta}_1(\theta_s, \phi_s) \boldsymbol{\Gamma}_s \mathbf{p}(\gamma, \eta) \right] e^{+jd_s} \\ \vdots \\ \mathbf{v}_M(\theta_s, \phi_s) \left[\boldsymbol{\Theta}_M(\theta_s, \phi_s) \boldsymbol{\Gamma}_s \mathbf{p}(\gamma, \eta) \right] e^{+jd_s} \end{bmatrix} \tag{16}$$

where $\boldsymbol{\Gamma}_s$ is a 2×2 random scattering matrix and d_s is the path length difference. The parameter ε determines the relative strength of the multipath component and N_{scat} is the number of scatterers. For the simulations, $\varepsilon = 10$ dB and $N_{scat} = 20$.

Table 1. Performance of calibration algorithms for a polarization-diverse array.

Algorithm	$\bar{\varepsilon}_\theta$ **(Deg)**	$\bar{\varepsilon}_\phi$ **(Deg)**
Conventional Calibration	0.77	0.40
Polarization Diverse Calibration	0.13	0.05

4.1. Discussion

For the study presented in this paper, simulations were performed using 200 calibration points randomly sampled over the set of data taken in 90° azimuth and 30° elevation sectors. The presented results are the average of 10 trials.

For comparison purposes, DF performance is evaluated for the following scenarios:

1. **Conventional array calibration:** DF is performed using conventional array calibration (6).
2. **Polarization diverse array calibration:** DF is performed using polarization diverse array calibration (11).

The root mean square error (RMSE) of the AOA estimation error is defined as

$$\bar{\varepsilon}_\theta = \sqrt{\frac{1}{K}\sum_{k=1}^{K}\left(\hat{\theta}_k - \theta_k\right)^2} \tag{17}$$

and

$$\bar{\varepsilon}_\phi = \sqrt{\frac{1}{K}\sum_{k=1}^{K}\left(\hat{\phi}_k - \phi_k\right)^2} \tag{18}$$

for azimuth and elevation errors, respectively, and is used to assess DF performance for the above scenarios.

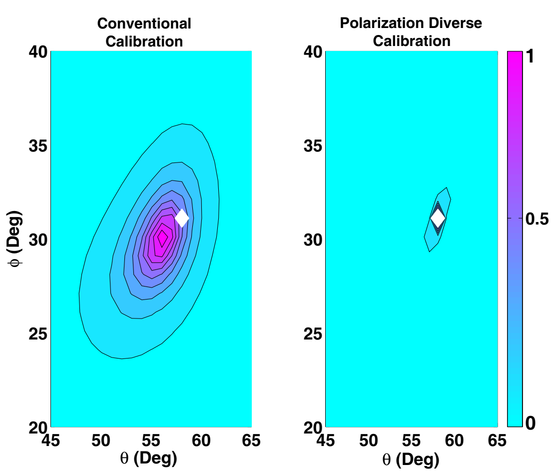

Fig. 3. Example DF spectra. The diamond represents the true source location.

Table 1 offers a quantitative algorithm performance comparison which verifies that significant performance gains over conventional array calibration algorithms are possible with usage of the proposed polarization diverse calibration algorithm. This is further corroborated in the example DF spectra in Figure 3. The diamond in Figure 3 represents the true peak location. The peak width when using the polarization diverse calibration algorithm is significantly narrower and closer to the true source location than when using conventional calibration. Furthermore, the promising results of the polarization diverse calibration algorithm indicates that it should not be the source of a performance bottleneck when used in an actual system.

5. CONCLUSION

Vector sensors are useful in applications where limited physical space necessitates sensor arrays with reduced aperture. Source-localization performance in the presence of sensor manifold perturbations was assessed for a configuration of multiple trimmed vector sensors applicable to a small aircraft. A novel polarization diverse calibration algorithm was developed and shown to yield a very significant performance improvement over calibration algorithms for conventional arrays.

6. REFERENCES

[1] A. Nehorai and E. Paldi, "Vector-Sensor Array Processing for Electromagnetic Source Localization," *IEEE Trans. Sig. Proc.*, vol. 42, pp. 376-398, Feb. 1994.

[2] E. Ferrara and T. Parks, "Direction Finding with an Array of Antennas Having Diverse Polarizations," *IEEE Trans. Ant. & Prop.*, vol. 31, pp. 231 - 236, Mar. 1983.

[3] K.T. Wong and M.D. Zoltowski, "Closed-form Direction Finding and Polarization Estimation With Arbitrarily Spaced Electromagnetic Vector-sensors at Unknown Locations," *IEEE Trans. Ant. & Prop.*, vol. 48, pp. 671 - 681, May 2000.

[4] H. Mir. et al, "Self-Calibration of an Airborne Array," *38th Asilomar Conf. Sig., Sys. Comp.*, pp. 2340-2344 , Nov. 2004.